Molecular QCA Design with Chemically Reasonable Constraints

MICHAEL CROCKER, MICHAEL NIEMIER, X. SHARON HU,
and MARYA LIEBERMAN
University of Notre Dame

In this article we examine the impacts of the fundamental constraints required for circuits and systems made from molecular Quantum-dot Cellular Automata (QCA) devices. Our design constraints are "chemically reasonable" in that we consider the characteristics and dimensions of devices and scaffoldings that have actually been fabricated. This work is a necessary first step for any work in QCA CAD, and can also help shape experiments in the physical sciences for emerging, nano-scale devices. Our work shows that QCA circuits, scaffoldings, substrates, and devices should all be considered simultaneously. Otherwise, there is a very real possibility that the devices and scaffoldings that are eventually manufactured will result in devices that only work in isolation. "Chemically reasonable" also means that expected manufacturing defects must be considered. In our simulations we introduce defects associated with self-assembled systems into various designs to begin to define manufacturing tolerances. This work is especially timely as experimentalists are beginning to work on merging experimental tracks that address devices and scaffolds—and the end result should facilitate correct logical operations.

Categories and Subject Descriptors: B.6.3 [**Logic Design**]: Design Aids—*Simulation*

General Terms: Design, Reliability, Verification

Additional Key Words and Phrases: Nanotechnology, quantum-dot cellular automata, defects, physical simulation

ACM Reference Format:

Crocker, M., Niemier, M., Hu, X. S., and Lieberman, M. 2008. Molecular QCA design with chemically reasonable constraints. ACM J. Emerg. Technol. Comput. Syst. 4, 2, Article 9 (April 2008), 21 pages. DOI = 10.1145/1350763.1350769 http://doi.acm.org/10.1145/1350763.1350769

This article is an extended version of the paper "Using CAD to Shape Experiments in Molecular QCA" in Proceedings of the International Conference on Computer-Aided Design (ICCAD'06), 907–914.

We thank NSF for supporting this work under CPA Grants CCF-0541234 and CCR-02-10153.

Authors' address: M. Crocker, Department of Computer Science and Engineering, University of Notre Dame; email: mcrocker@nd.edu.

1. INTRODUCTION

It is hardly necessary to discuss why it is important to look at computational systems that are not based exclusively on CMOS transistors. Emerging technologies have the potential to offer their own unique "wins." Quantum computation can potentially factor very large numbers efficiently, arrays of nanowires might offer very dense memory, and spin-based systems could provide nonvolatile storage and low power operation. This work looks at systems of molecular Quantum-dot Cellular Automata (QCA) devices. We consider statistical mechanical analyses of how the fundamental constructs required for computationally interesting circuits might function in the presence of chemically reasonable fabrication constraints.

At least at the device level, molecular QCA cells could overcome the obstacles of interconnect and power dissipation that molecular transistors cannot. QCA [Tougaw and Lent 1994] accomplishes logical operations and data movement via Coulombic interaction rather than with electric current flow. A theoretical analysis of a molecular implementation has shown that QCA-based circuits could potentially be clocked at extremely high frequencies [Timler and Lent 2002],[1] potentially lead to circuits with densities that are several orders of magnitude beyond what end-of-the-curve CMOS can provide [Chaudhary et al. 2005], and dissipate little power [Timler and Lent 2002]. Experiments have shown a molecule is capable of switching between configurations that represent binary 0 and 1 states [Qi et al. 2003].

QCA cells interact as the charge configuration of one cell alters the charge configuration of the next cell. Because electrostatic interactions are strongly distance-dependent, the smaller the QCA devices can be made, the better they work. Also, information transmission and processing is carried out by the same entities—QCA cells—rather than by separate devices and wires. In CMOS, the preponderance of real estate on chip is taken up by *wires*, so shrinking CMOS devices does not necessarily produce corresponding gains in *device* density. When smaller QCA cells are made, QCA interconnect shrinks too.

Numerous efforts have also looked at design issues for various implementations of QCA. In particular [Chaudhary et al. 2005] has addressed implementable interconnect for molecular QCA. This work assumed self-assembling systems based on the DNA tiles proposed by Seeman and Winfree. According to Chaudhary et al. [2005], one consequence of this potential fabrication mechanism was that a co-planar wire crossings would be difficult to fabricate. The work was important because it showed that alternative interconnection mechanisms should not adversely affect area. As a result, the milestone of fabricating a coplanar wire crossing could probably removed from the physical science critical path.

This work is related to Chaudhary et al. [2005], but takes an important step *back*. We consider via statistical mechanical analysis not just whether the structures required for the methods proposed in Chaudhary et al. [2005] will function properly, but whether a functionally complete logic set will function

[1]Switching times will ultimately depend on the capabilities of the CMOS circuitry.

properly if existing devices and current candidate scaffoldings are used to build it. It will also lay the foundation for any other future work in QCA CAD—helping to quantify important metrics such as wire pitch, the number of devices that can be active simultaneously and redundancy required for defect tolerance.

There is a belief held by some nano-scale device researchers that "it is premature to consider any design-related work until devices and substrates have been experimentally realized." The results of our work demonstrate that design plays an important—and necessary—role. Devices and scaffoldings are not the only milestones on the critical path to a realizable, nano-scale system. If architectures, viable interconnect, defect tolerance, etc. cannot be addressed, the end goal of a system is still not met. Moreover, in this article, we will show that if molecular QCA devices and scaffoldings are in fact considered independently of circuits and systems, we could end up with a combination of devices and scaffoldings that *look* like circuits, but do not function like circuits. Without a close coupling between all 3 threads (circuits, scaffoldings, and devices), work in any individual thread would be fundamentally incomplete.

We begin in Section 2 by discussing relevant background. We discuss QCA simulation tools in Section 3. In Section 4, we outline practical simulation parameters that correspond to experimental results relevant to molecular QCA devices. We describe a statistical mechanical analysis of a functionally complete logic set given two candidate molecules in Section 5, how defects might affect logic in Section 6, and how a DNA scaffold might affect logic in Section 7. Section 8 concludes.

2. BACKGROUND

2.1 Implementation Independent Fundamentals

QCA represents information by encoding binary numbers in cells that have a bistable charge configuration. A QCA cell can consist of 2 or 4 "charge containers" (i.e., quantum dots) and 1 or 2 excess charges, respectively. One configuration of charge represents a binary 1, the other a binary 0 Figure 1(a). Figures 1(b)–(d) illustrates a fundamental set of QCA circuit elements [Tougaw and Lent 1994]. The majority gate (Figure 1(b)) implements the logic equation $AB + BC + AC$. The output cell assumes the polarization of the majority of the 3 input cells. Note that permanently setting one input of a majority gate to a 0 or a 1 yields an AND or OR gate respectively; signal inversion is also possible (see Figure 1(d))—hence we can form a functionally complete logic set. A QCA wire (Figure 1(c)) is just a line of QCA cells; at the input end, one cell must be polarized to act as the driver for the wire. QCA wires with different orientations (Figure 1(e)) can the cross in the plane without the destruction of the binary value on either wire. A signal on a 45-degree wire will alternate between 1 and 0; values can be transferred between wire types [Tougaw and Lent 1994; Lent and Tougaw 1997].[2]

[2]It is worth noting that [Blair 2003] and our simulations show that by adding redundancy at the device level, the constructs in Figure 1 should be more resilient to errors/defects (i.e., using a wire that is 2 cells thick instead of 1 cell thick).

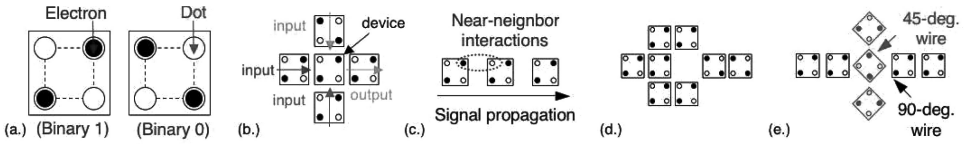

Fig. 1. "Cartoon" representations of (a) a 4-dot QCA cell, (b) a majority gate, (c) a wire segment, (d) an inverter, (e) a QCA physical wire crossing.

A "clock" structure turns devices on/off and provides gain. The clock causes groups of QCA cells to transition from a null state (off) to a bistable, active state (1 or 0), and then back to a null state. For systems of molecular QCA cells, the clock would essentially be a continuously propagating electric field that would move a computation across a layer of QCA devices. Computation would occur at the leading edge of a wave front as a cell is turned on. The electric field pushes charge up to the active state (providing gain) while a driver—a cell that is already on and polarized—determines if the cell just turned on will be a 1 or 0 . The phases of a clock signal could take the form of time-varying, repetitious voltages applied to CMOS wires embedded underneath a QCA circuit. Four wires—associated with four clock phases—are required in order to generate smooth and continuous field propagation [Hennessy and Lent 2001]. A different bit of data could be associated with every four wire group. Cells are not clocked individually. From an architectural perspective, this results in a certain amount of inherent pipelining determined by the granularity of the clock structure [Niemier and Kogge 2001].

2.2 Molecular QCA Primer

2.2.1 *Devices.* QCA devices (and circuits) have actually been made from metal [Amlani et al. 1998; Snider et al. 1999] and from magnets [Imre et al. 2006], but can also be made from a single chemical molecule. Molecular QCA cells correspond to a class of compounds called *mixed-valence compounds*, which contain multiple redox centers in different oxidation states. For a molecular QCA device, each "quantum dot" or "charge container" would be a single redox center, and the redox centers would be rigidly held together by covalent bonds [Qi et al. 2003]. A recent experiment demonstrates that applying reasonable electric fields (like from a clock structure) can move a charge between two sites of a molecule engineered to function as a two-dot QCA cell [Qi et al. 2003]. Thus, experimental results show molecules that act as QCA devices, switching between a chemical representation of a binary 0 and a binary 1. This is important both as a basic demonstration that molecules can be used as containers for mobile charges, and as a prototype for the clocking of QCA molecules by pulling charges down to a null position from an active QCA layer. Four-dot QCA molecules have also been made [Jiao et al. 2003]. Our work will look at logic in the context of 4-dot QCA molecules Figure 2(a).

2.2.2 *Making Circuits.* The requirements for positioning molecular QCA cells are stringent. Molecules must be placed in specific locations with nanometer precision. This work will begin to explain exactly what precision is necessary

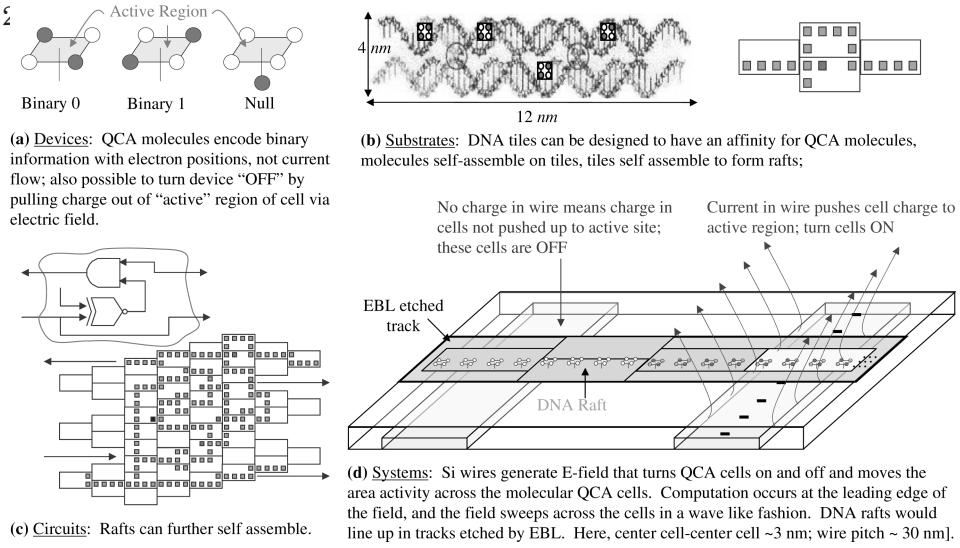

(a) Devices: QCA molecules encode binary information with electron positions, not current flow; also possible to turn device "OFF" by pulling charge out of "active" region of cell via electric field.

(b) Substrates: DNA tiles can be designed to have an affinity for QCA molecules, molecules self-assemble on tiles, tiles self assemble to form rafts;

(c) Circuits: Rafts can further self assemble.

(d) Systems: Si wires generate E-field that turns QCA cells on and off and moves the area activity across the molecular QCA cells. Computation occurs at the leading edge of the field, and the field sweeps across the cells in a wave like fashion. DNA rafts would line up in tracks etched by EBL. Here, center cell-center cell ~3 nm; wire pitch ~ 30 nm].

Fig. 2. A brief vision of a DNA-based QCA system. (a) Molecular Devices, (b) DNA Substrate Rafts, (c) Circuit Self-assembly, (d) DNA system with clocking wires.

to make QCA circuits. Recent results in DNA tiling suggest that DNA could be used as a "circuitboard" to position QCA cells. One viable target assumes DNA tiles fabricated by Seeman and Winfree [Winfree et al. 1998] as the scaffolding. QCA molecules would attach covalently to modified DNA nucleotides (Figure 2(b)). Assuming the tiles retain the B-DNA duplex, sites in the major groove could serve as attachment points with a periodicity of 3.6 Angstroms along the helix axis, and 2 or 4 Angstroms perpendicular to the helix axis (resulting in device densities of up to $10^{13}/cm^2$.) This work has significant critical mass as many research groups are currently looking at creating and attaching nano-particles to DNA-based scaffoldings [Labean et al. 2005; Rothemund et al. 2004; Rothemund 2005]. Thus, DNA has the *potential* to act as a circuitboard, be made large enough to hold computationally interesting circuit components, and be built with reasonable yields. It should also be possible to enforce extremely rigid cell orientation on the DNA tile—which is good for a 4-dot molecular QCA cell. There are good precedents for rigid placements of metal complexes on duplex DNA [Hurley and Tor 2002].

2.2.3 *Making Systems.* Large DNA structures with molecules attached to them could be "guided" to certain places to form more complex circuits (Figure 2(c)). Directed assembly envisions using 10–100 nm, top-down lithography to guide the attachment of circuitboards to silicon substrates. Interactions between the circuitboards and ordered pads with matching shapes will allow them to dock at certain locations on a surface with specific partners. DNA hybridization between circuitboards will maintain sub-nm registry from one circuitboard to the next. [Hu et al. 2005] shows that silicon is a viable substrate for guided DNA tile binding. With the DNA circuitboard attaching to a silicon substrate, metal clocking wires underneath can drive the system (Figure 2d).

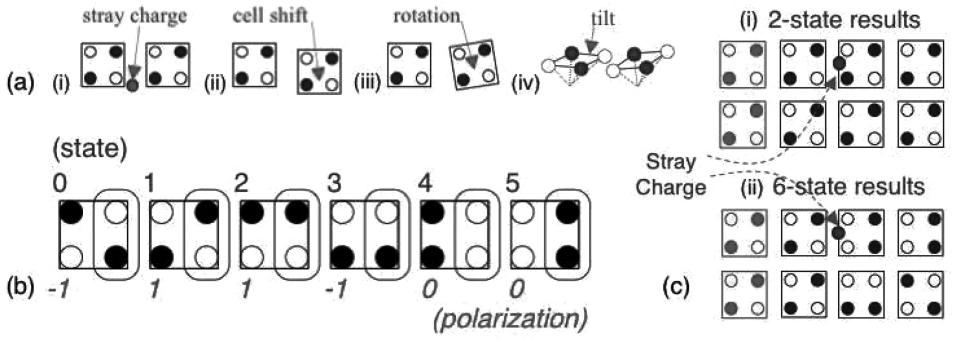

Fig. 3. (a) Expected defects, (b) Possible states of a QCA molecule and "seen" polarizations, (c) Defects may cause degenerate states.

2.3 Fabrication Challenges

Realistically, any nano-scale fabrication process will not be defect free. Stray charges (Figure 3(a)(i)), cell shifts (Figure 3(a)(ii)), cell rotations (Figure 3(a)(iii)–(iv)), and missing cells might all cause a circuit construct to produce the wrong result. While (experimentally) no group has attempted to deterministically place individual QCA molecules, there is more than ample evidence to justify these assumptions. As one example, Le et al. [2004] look at attaching gold nano particles to a DNA scaffold. The AFM imagery in Le et al. [2004] illustrates that some particles are either missing or misaligned. While these problems could be caused by perturbation from the AFM tip, incomplete hybridization between the nanoparticles and the DNA scaffold is the most likely source of missing particles, and the relatively floppy duplex DNA used to attach the particles to the DNA scaffold is the most likely source of particle misalignment. Another defect of particular concern is stray charge, which could come from a scaffolding molecule (i.e., the sugar-phosphate backbone of DNA) or from the substrate surface (i.e., the ionizable silanol groups on silicon native oxide).

2.3.2 *Implementable Interconnect.* Implementable interconnect presents near-to-midterm challenges to system designers. While enforcing one cell orientation appears possible [Hurley and Tor 2002], creating a circuit part that has cells with two different rotations (i.e., on the same DNA tile), is a much more difficult task to experimentally solve. While not impossible, a first implementation target will probably be a system that has cells with just one orientation. Thus, the coplanar wire crossing shown in Figure 1(e) would not be available for any design. Still, in the worst case, selective duplication and logical crossings should be satisfactory in terms of implementation and performance [Chaudhary et al. 2005]. Here, we consider the parts needed not just for interconnect, but also for a functionally complete logic set—using the chemically reasonably constraints just discussed.

3. METHODOLOGY

We will use simulation to study how a functionally complete logic set made from misplaced QCA devices might function.

3.1 Existing Simulators

QCA Designer [Walus et al. 2003] and M-AQUINAS [Blair 2003] both simulate systems of multiple QCA devices. Both simulators allow a user to specify attributes such as cell size, cell spacing, etc. However, they also only allow a device to be in 3 possible states—a 1 or 0 when the cell is active, or a null state when the device is clocked off. With a 4-dot molecular device there are really 6 possible states that a device might be in when active (see Figure 3(b)). Although states 2–5 are higher in energy than states 0 and 1, they still need to be included for completeness.

It is unlikely that a single, isolated QCA cell would settle into any of the four degenerate cases (2–5 in Figure 3(b)). With a square molecule, simple trigonometry tells us that the electrons would be farthest from each other when in opposite corners, thus minimizing the total energy of the "system." However, when many QCA cells are placed in close proximity to one another to form a circuit, it is possible that a higher local energy state might be favored because it reduces the energy of the entire QCA circuit—and one of the four degenerate cases might occur.

3.2 Statistical Mechanical Simulations

Our goal is to investigate how well the components needed for a functionally complete logic set and implementable interconnect will function assuming a 4-dot QCA molecule with nanometer dimensions and the scaffolding discussed in Section 2.2. While we will leverage M-AQUINAS (as it supports continuous clocking), our results and analysis are primarily based on statistical mechanical simulations. We have extended the work of Ungarelli et al. [2000] and Wang and Lieberman [2004] by adding counter ions to the simulation in order to maintain charge balance in the QCA molecules, and by augmenting the code to study the potential defects discussed above. Our analysis considers electrostatic forces and potentials between all point charges in a circuit. Such calculations are performed for all possible combinations of cell states. The end goal is to use the energy potentials to determine with what probability a circuit will behave correctly, and how "stable" it is.

It is important to note that our simulator does not assume a clock. In a sense, this is the most "pessimistic" simulation possible. In addition to providing gain, a continuously propagating clock also prevents some potential metastable states from occurring. Certain configurations of cells that could settle into a metastable state will never have the opportunity to interact—as they will never be active simultaneously. However, a clock wave is relatively large when compared to cell size. Thus, a column of active cells will be more than one cell wide, and a statistical mechanical analysis is a good way to model this situation. If an unclocked statistical mechanical analysis of a circuit element shows a high probability of correct output, it should certainly function properly in conjunction with a clock.

We cycle through all possible combinations of QCA cell states and sum up the total energy associated with each state. An n-body energy calculation is made between all electrons and counter ions for each combination. The energy

potential between any two charges m and n is found with Equation (1).

$$E_{m,n} = \frac{q_m q_n}{4\pi\epsilon\, r_{m,n}}, \tag{1}$$

A counter ion has an opposite charge equal to two electron charges ($q = -2e$). All 6^N combinations of cell states are considered, and the sum for each state combination, i, is calculated with Equation (2).

$$E(i) = \sum_{m=1}^{N-1} \sum_{n=m+1}^{N} E_{m,n}, \tag{2}$$

The state combination with the lowest energy sum is denoted by $E(ground)$. This ground state is used to find the energy difference, $\Delta E(i)$, for each combination as shown in Equation (3). Note that ΔE of the ground state will be 0.

$$\Delta E(i) = E(i) - E(ground), \tag{3}$$

Still, it is insufficient to simply determine the ground state. In order to ensure that the behavior demonstrated in the ground state is valid, a stability test must be completed. The result of this stability test is a probability ratio that indicates how likely it is that the ground state behavior will match the overall circuit behavior. The Boltzmann equation provides a useful stability measure. For each of the 6^N combinations there is an energy difference $\Delta E(i)$, which is necessary for the Boltzmann energy calculation. (As excited states can be thermally populated we incorporate temperature into our statistical mechanical analysis.) By summing the Boltzmann energies for all 6^N combinations, the partition sum F_{total} can be found. This partition sum is the first part of the probability ratio.

$$F_{total} = \sum_{i=1}^{6^N} e^{\frac{-\Delta E(i)}{kT}}, \tag{4}$$

A similar sum is calculated for each of the 6 possible outputs (i.e., the states in Figure 3). The output cell of each combination has a specific state, j, between 0 and 5. All combinations with the same output cell state are grouped together. Next, the same Boltzmann calculation is performed for all combinations in the same group, and the sum is kept as F_j. This is done for all output states, $j = 0 - 5$.

$$F_j = \sum_{i=1}^{6^N} e^{\frac{-\Delta E_j(i)}{kT}}, \tag{5}$$

Now that we have the Boltzmann sum for all combinations, F_{total}, and the Boltzmann sums for each possible output cell state, F_j, the stability ratio can be computed for the ground state. Using the output cell of the ground state, the probability is calculated. If the output cell state is k, then the probability that the ground state's behavior will match the overall circuit behavior is found by the ratio of F_k to F_{total}. The ratio is calculated for all k.

It is also useful to know the output cell's expected value. We can calculate this by using the Boltzmann partition sums and the output polarizations of a

given cell state (see Figure 3(b)). Note that the polarization value is defined as the difference between the rightmost occupancy of the top and bottom electron wells of the cell. The sums F_j are weighted with the corresponding polarization value, summed, and divided by the total partition sum, F_{total}. Both F_0 and F_3 are multiplied by -1, F_1 and F_2 are multiplied by 1, and F_4 and F_5 are multiplied by 0. The expected value results in a polarization between -1 and 1. In some situations, the most probable output may not match the ground state's output.

As just one example of why this more detailed, 6-state analysis is necessary, we briefly discuss the simulations captured by Figure 3(c)—a short wire segment with some device-level redundancy (the distance between redox sites is 1 nm and the center-to-center spacing between cells in the x or y dimension is 2 nm). However, we also introduce a stray charge into this configuration. When this arrangement of cells was simulated with a 2-state statistical mechanical model, simulation results showed that the wire would behave as shown in Figure 3(c)(i)—i.e., the binary 1 at the input would propagate to output with a near 100% probability. However, when the exact same simulation was run assuming a 6-state model, the ground state of the system was that shown in Figure 3(c)(ii). Only when the stray charge was moved at least 0.66 nm away from the plane of the devices, did the ground state resemble Figure 3(c)(i). Stray charges and other defects (rotated cells, shifted cells, etc.) might cause these degenerate states and they should be included for completeness.

4. SIMULATION PARAMETERS

Several candidate QCA devices have been made. The distance between redox centers for the molecule discussed in Jiao et al. [2003] is essentially 0.6 nm. A ruthenium-based Creutz-Taube ion [Creutz and Taube 1973] was synthesized to be used as a molecular QCA cell (to combat undesirable counter ions). The CT ion has two electrochemically reversible and chemically stable redox centers, and a strong coupling between them to allow for tunneling of the charge that will represent a binary 1 or 0. The distance between redox centers for the Creutz-Tabue ion is 0.9 nm. Larger molecules have also been made. In an effort to "summarize" the range of spaces, we will consider 4-dot QCA molecules with 0.9 nm and 1.5 nm between redox sites in this section.

For center-to-center spacing, we initially do not target any of the patterning mechanisms discussed earlier. Instead, we make this a variable to gain insight as to the ideal spacing for two candidate molecules. Later, we consider a candidate DNA scaffold—where sites in the major groove of a DNA tile could have a periodicity of 3.6 nm along the helix axis, and 2 or 4 nm perpendicular to the helix axis. To study the effects of defects on logic, we have chosen a 1 nm edge-to-edge spacing (on the order of what we would like, but also a distance that is plausible) which leads to the aforementioned 1.9 nm center-to-center spacing. An unchanging center-to-center spacing will also allow us to consistently evaluate the effects of defects.

In addition to testing different sizes and spacings, our simulations will also look at device-level redundancy. At the device level, circuits can be made with

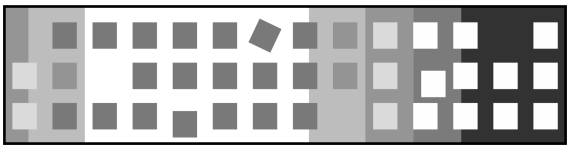

Fig. 4. A QCA wire can be made three devices thick. This redundant design causes the resulting circuits to be more tolerant of defects. The dark squares are active devices successfully transmitting a logic 1 value on a defective wire as the clocking field in white passes along the wire.

thicker parts (see Figure 4). Thicker wires are more tolerant of fabrication defects [Blair 2003]. Thus, while a wire that is one device thick may not transmit a logical value successfully if devices are missing or rotated, simulations show that a wire that is three devices thick, for example, would transmit a logical value successfully even with defects present (Figure 4).

5. SIMULATIONS OF A FUNCTIONALLY COMPLETE LOGIC SET

Here, we present a statistical mechanical analysis of the fundamental circuit constructs needed for a functionally complete logic set and implementable interconnect as discussed in Chaudhary et al. [2005]. Specifically, we consider: (1) 6 active states, (2) ideal scaffolding dimensions, and (3) QCA molecules with reasonable dimensions. DNA scaffolding dimensions will be considered in the next section. Majority gates, inverters, and wire segments, all a single cell "wide," are studied—enough to realize a functionally complete logic set and implementable interconnect. Redundancy at the device level is also addressed. Note that our simulations consider the full truth table for each construct. (The probabilities of a correct output associated with each input combination are averaged).

In Figure 5, contour plots report the probability of a correct output for various circuit constructs as a function of center-to-center cell spacing. All simulations assume room temperature operation (i.e., 300K). Figures 5(a)–(b), (c)–(d), and (e)–(f) report the probability of a correct output for a majority gate, inverter, and wire segment, respectively. All constructs have no device-level redundancy and are thus one cell thick, except for Figure 5(f) which contains results for a three cell wide wire segment. A distance of 0.9 nm between redox sites is used for Figures 5(a),(c),(e), and (f), while Figures 5(b) and (d) assume 1.5 nm redox spacing. Figures 5(a)–(b), (c)–(d) illustrate how the probability of a correct output is affected as the center-to-center distance between devices changes, but for different sized molecules. Cell spacing in the x and y dimensions is plotted along the x and y axis; the probability of a correct output corresponds to a shade of grey in the contour plot. This study provides insight into how the distance between redox sites affects ideal scaffolding size. Figure 5(e) and (f) provide insight as to how device level redundancy affects the probability of a correct output.

We discuss ideal scaffolding spacing first and note that QCA molecules could be placed too closely together. For every circuit with cells in more than 1 row, there is a region in the contour plot (for low x and y values) that indicates a low probability of a successful output. An example is shown in the insert of Figure 5(a)—derived from assuming 0.9 nm redox spacing and 1.2 nm center-to-center cell spacing. Thus, there are just 0.3 nm between cell edges.

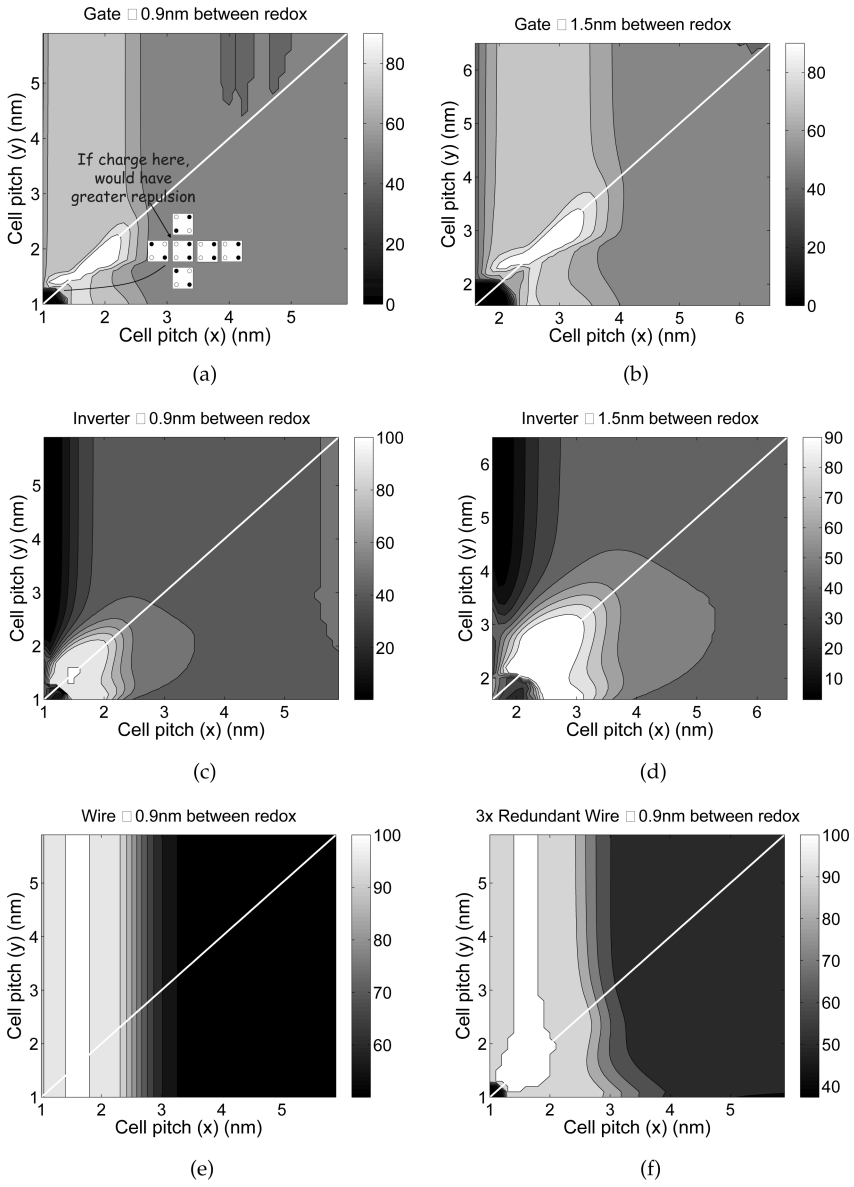

Fig. 5. Probability of a correct logical output as a function of cell spacing. Graphs (a), (c), and (e) look at majority gates, inverters, and wires (all 1 cell thick) with 0.9 nm between redox centers. Graphs (b) and (d) look at majority gates and inverters for a larger molecule (1.5 nm between redox sites). Graph (f) looks at a wire segment 3 cells thick with 0.9 nm between redox sites.

Table I. Ideal Center-to-Center Cell Spacings for Logic Family with 0.9 nm Between Redox Sites

Construct	Min. Space (nm)	Max. Space (nm)
1× Wire	1.0×10^{-9}	2.5×10^{-9}
1× Inv	1.3×10^{-9}	2.1×10^{-9}
1× Gate	1.5×10^{-9}	2.3×10^{-9}

If devices are placed too close together, the distance between redox centers is greater than the distance between device edges. The electrostatic coupling between redox centers of adjacent molecules is tighter than the coupling between the redox centers within the cells themselves, and charges have a tendency to "flee." Also, as the distance between molecules increases, the probability of a successful output also drops—as electrostatic interactions fall off as the distance between charges increases.

It should be fairly obvious that there is also a "sweet spot" (or ideal cell spacing) for each circuit construct. We consider this further by looking at the graphs in Figures 5(a), (c), and (e). The most important question to consider is whether or not the "sweet spots" for each fundamental circuit construct have any overlap. If so, this means that, at least theoretically, there is a "universal" scaffolding that should allow *all* of the constructs for a functionally complete logic set to function correctly. For the constructs in Figures 5(a), (c), and (e), the minimum and maximum center-to-center cell spacings (assuming a square grid) are reported in Table I.

One can see that center-to-center spacings ranging between 1.5×10^{-9} and 2.1×10^{-9} nm should work well for every construct. However, placement does not have to be this precise. Uneven grid spacings can still provide correct outputs. To gain more insight, we examined the raw data used to construct Figures 5(a), (c), and (e), and considered only the cell spacings that gave a probability of correct output that was above 85%. (More will be said about acceptable probabilities in the next section.) In many cases, the grid spacings between successful gates, wires, and inverters does not have to be the same and can vary by at least 0.4–0.5 nm and still be above the 85% threshold (1.5 nm in the x and 1.0 nm in the y dimension is an example).

There appears to be a rough linear relationship between the spacing between redox sites and ideal center-to-center cell spacings. The graphs in the first and second rows of Figure 5 have similar shapes. For a molecule with 1.5 nm between redox sites, the ideal range for all circuit constructs is 2.1–2.9 nm assuming a square grid. Again, for many cases, spacings can vary by 0.4–0.5 nm.

Increasing the device level redundancy also has a positive affect on the probability of seeing a correct output. This is more important when defects are introduced—as will be discussed in detail in Section 6. However, we note that the number of times that a wire segment produces the correct output (with high probability) increases as wire thickness increases, for example.

The above results are important for two reasons. First, they show that for existing molecules, there is a scaffolding that will facilitate the correct operation of all of the components needed for a functionally complete logic set and interconnect. Second, while we can use this information to target an ideal

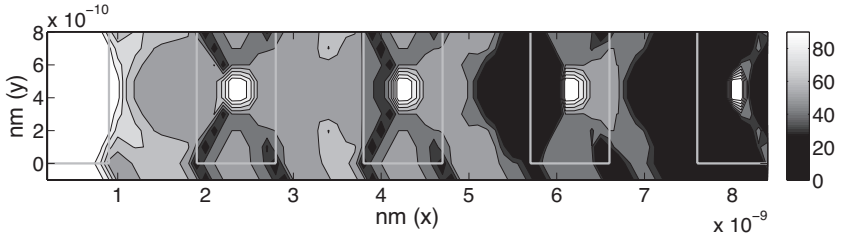

Fig. 6. Effects of stray charge on a wire.

scaffolding, we can also use these results to target an ideal molecule. (It may be easier to construct a device that conforms well to a more easily fabricated scaffolding.) We consider one candidate—DNA tiles—in Section 7.

6. DEFECTS

In this section we consider how stray charges, shifts and rotations will affect logic. Rotation defects in 3D, also called tilt defects (Figure 3(a)(iv)), are not included.

6.1 Stray Charge

We begin by analyzing how stray charges will affect the circuit constructs needed for a functionally complete logic set. All of the simulations that will be discussed here—and throughout the article—were conducted assuming room temperature operation (300K). Also, all simulations considered all possible input combinations for each configuration tested. Thus, if we simulate how a wire segment would be affected by a stray charge in a specific position, both 0 and 1 inputs were applied, the probabilities were recorded, and then averaged.

6.1.1 *Distance Away from the Plane.* We first consider how a single stray charge might affect a majority gate, wire, and an inverter with no device-level redundancy. A single charge was placed at various distances away from the plane and moved in 0.1 nm increments in both the x and y dimensions over the design. Each time the charge was moved we calculated with what probability a given circuit construct would produce the correct logical output.

These simulations allowed us to generate contour plots like the one that appears in Figure 6 (here a 5 cell wire segment is shown). The color of the plot is indicative of whether or not the circuit would produce the correct output if a stray charge were at that particular point. For example, in Figure 6, the region around the point (5.6 nm, 0 nm) is dark—indicating a low probability of a correct output if a stray charge were present in the plane of molecular redox sites in this position. This makes sense because if a cell should be polarized as a 1, there would be two negatively charged particles in the same space—most likely inducing a mistake state. If the charge is not in the plane of a molecule's redox sites (i.e., it is 1.0 nm away), the probability of seeing a correct output increases significantly (the contour plot would be almost completely white indicating a high probability of a correct output in all cases). This is good because from

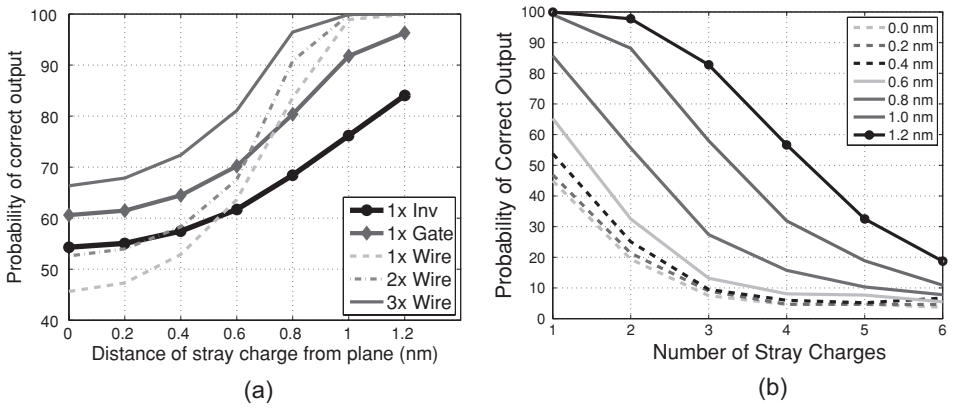

Fig. 7. (a) Effects of a single stray charge, (b) Effects of multiple charges.

a fabrication standpoint, this is actually quite realistic. For example, for the synthesized 4-dot QCA molecule discussed in Jiao et al. [2003], the redox sites are suspended in the xz-plane by a strut that would attach to a scaffold. This distance can be a design parameter. Additionally, charge is anticipated to be in the scaffold below the active plane.

Rather than display contour plots for the other simulated circuit constructs, we have summarized our results in Figure 7(a) by simply averaging the probabilities used to construct the contour plots in Figure 6. Also, inverters and majority gates behave well as a stray charge moves away from the plane of the devices. The construct most susceptible to a stray charge appears to be the inverter where the probability of seeing a correct output is approximately 84% when the charge is 1.2 nm away from the plane.[3]

6.1.2 *Redundancy.* We also wanted some insight as to how device-level redundancy would combat the effects of a single stray charge. As a result, we repeated the experiments discussed above for a wire segment that was 2 and 3 cells thick. These results are also reported in Figure 7(a). As expected, device-level redundancy does increase the probability of seeing a correct output.

6.1.3 *Multiple Stray Charges.* We now consider how circuit constructs might be affected if multiple stray charges are present. For this study we looked at the circuit construct (with no redundancy) that was most *tolerant* to a single charge (the wire segment) as this should set the bar for the best behavior that we might expect. As before, stray charges were placed at different distances away from the plane of the redox sites. Between 1 and 6 stray charges were randomly placed in the circuit and each configuration was tested with both 0 and 1 input values. Results are reported in Figure 7(b); each point is the average of 1000 simulation runs.

[3]84% is not necessarily bad. We have done some work to correlate clock driven simulations to statistical mechanical simulations. Some constructs that statistical mechanics reported would function properly about 60% of the time worked well in a clocked system. However, this was for a 2-state device model [Niemier et al. 2006]. Clearly, further study—and device-level redundancy—is needed.

At first glance, wire segments in the presence of multiple stray charges—even stray charges away from the plane of the redox sites—do not seem to perform well. As the number of charges increases, the probability of seeing the correct output drops. To understand why this was happening, we examined the individual data points used to create the averages reported in Figure 7(b). Invariably, in configurations with a low probability of a correct output, 2 charges usually appeared very close together.[4] What this means is that some cell in the wire was usually influenced by a charge that was twice that of a single electron. Additionally, even when the probability of seeing a correct output was average (i.e., approximately 50%), this usually occured because the stray charge configuration caused the wire to be stuck at a 0 or 1—essentially rendering it useless for transmitting data.

Our first thought for combating this problem was to increase device-level redundancy. To test this idea, we simulated wire segments that were three cells long and one, two, and three cells thick. Three and four charges were randomly placed in the design at a distance of 1.0 nm from the plane containing the redox sites. Again, the results of 1000 simulations were averaged. As wire thickness increased, the average probability of that wire segment producing a correct output increased by about 16–17% for each extra cell of thickness. However, increasing device-level redundancy also increases circuit area—and the number of stray charges could increase too! In short, if stray charges are distributed regularly, redundancy should help. If the distribution is more random with larger "clumps" of charge, device-level redundancy may be less likely to increase the probability that we will see a desired logical output. Fortunately, there is reason to believe that charges will not "clump" as electrostatic repulsion would tend to space them apart. However, a careful analysis of any potential substrate is essential.

6.2 Rotation

We next consider how circuit constructs might be affected by device rotations. The goal of this study was to determine by how much a cell could be rotated and still produce the correct logical output.

Our first set of simulations looked at wire segments with varying degrees of redundancy. The output cells of each segment were rotated between 0 and 45 degrees. Results are reported in Figure 8(a). Wire segments function quite reliably. For the inverter and majority gate, three of the devices in each construct were individually tested (cells 1–3 in the inverter in Figure 1d and an input cell, device cell, and the output cell for the majority gate). The probabilities reported in Figure 8(a) are averages of these simulations (no cell had a more significant effect than any other). Both of these constructs also perform well if a device is rotated (the inverter can seemingly tolerate 16–20 degrees of rotation while the gate can tolerate 21–25 degrees).

Our second simulation set attempts to understand what would happen at the logic level if a given device deposition mechanism only allowed rotation to

[4]For these simulations, this happened relatively frequently as our wire segment was only approximately 1 nm high and 9 nm long.

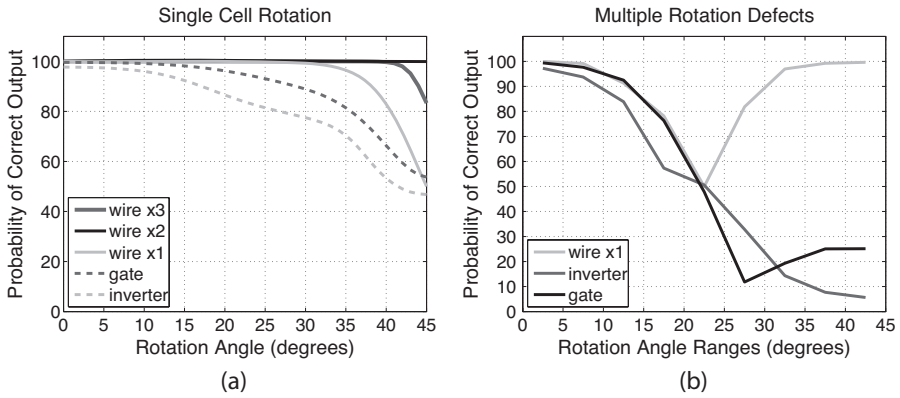

Fig. 8. (a) Effects of rotating one cell, (b) Effects of rotating all cells.

be controlled within a certain range. To test this idea, for each construct in Figures 1(b)–(d), we rotated *every cell* a random amount within some "bucket" and recorded the probability of seeing a correct output. Results in Figure 8(b) are the averages of 1000 simulation runs. (Values on the x-axis are meant to be bucket ranges, not individual data points.) Note that these experiments were conducted in three different ways: every cell was rotated by $+x$ degrees (i.e., between 0 and 5) $-x$ degrees (i.e., between 0 and -5) and $+/-x$ degrees (i.e., between 0 and 5 *or* 0 and -5). (The $+x$ data was used to construct Figure 8(b)). With one minor exception, there was no significant difference between each of these options. As one can see, each circuit element appears reasonably tolerant to rotations in the xz-plane to at least 11–15 degrees. Like before, the inverter is most susceptible to fabrication error.

Before continuing, we briefly discuss some of these trends in a bit more detail. First, as the size of allowable rotation increases, some circuit constructs actually begin to perform better. We will explain by example and more closely examine the v-shaped "wire x1" curve in Figure 8(b) and the coplanar crossing in Figure 1(e). For the 41–45 degree bucket, we are essentially simulating the wire with rotated cells that appears in Figure 1. Furthermore, because our simulated wire has an odd number of cells (5), and the polarization of a 45-degree wire should alternate from one cell to the next, the probability of seeing the correct output is very high. Second, this trend is not observed when each cell can be randomly rotated in the plus or minus direction. When these results were plotted (not shown) all curves essentially saturated at 50%. There was enough disorder in the wire that the probability of seeing the correct output was essentially an even chance. However, all constructs performed well until the 16–20 degree bucket.

6.3 Shifts

Cell shifts were also studied. The constructs in Figures 1(b)–(d) were again considered and each cell was randomly shifted by 10% of the distance between molecular redox sites in any direction. This 0.9 Å shift is much larger than

Table II. Effects of Shifts

	1× gate	1× Inv	1× wire	2× wire	3× wire
Prob.	92.18	89.16	99.76	99.96	99.99

shifts which might be caused by vibrational motions of the cells on the surface. Results are reported in Table II (again the averages of 1000 simulation runs) and are consistent with other defects. Cell shifts appear to have little affect on a logical output.

7. THE EFFECTS OF A DNA SUBSTRATE

Using DNA as a scaffolding for QCA systems is seemingly a natural fit—as it forms a "grid" that would allow for center-to-center spacings that are in the range of what appears to be ideal (a few nm). However, DNA tiles may form a "grid" that is not square. Recall that groove sites may be 3.6 nm apart in the x dimension, and 2.0 nm apart in the y-dimension. We will study how this affects a functionally complete logic set.

As our scaffolding attachment points are fixed, here we will vary the spacing between redox sites in an effort to determine the ideal sized molecule for this scaffolding. The probabilities with which wire segments and majority gates (with no device level redundancy and 2x redundancy) will produce the desired output are reported in Figures 7(a) and 7(b), respectively. (Inverters were also simulated, but these results are not illustrated). The interesting peaks in Figure 7(b) are the result of averaging the circuit stability for all 8 inputs combinations to the majority gate while the horizontal and vertical spacings are varied.

Based on these simulation results we can make the following observations. First, it appears that smaller molecules (i.e., 0.9 nm between redox sites) and a DNA scaffolding with the aforementioned dimensions are not a good match. When the distance between redox sites is 0.9 nm, the probability that a wire, inverter, and majority gate will produce the desired output ranges between 50–60%—even with additional device-level redundancy. If we assume a molecule with 1.5 nm between redox sites, the probability of a wire segment functioning correctly increases significantly—to almost 100% for varying degrees of thickness, but only to 65–70% for majority gates and inverters. (This makes sense as the dimensions of DNA are much closer to the ideal dimensions for the 1.5 nm molecules as seen in Section 5).

We believe that these lower overall probabilities occur because grid spacings are not square and there can be a greater interaction between cells in one dimension, than cells in all dimensions. Also, for the smaller 4-dot molecule, as cell spacings increase, the electrostatic interactions decrease. Still, this does not mean that DNA should not be considered as a scaffolding for molecular QCA devices. From a systems stand point, there are still other factors that we must consider.

One is to make the DNA grid more square. We may have little control over the spacing between groove sites, but we do not have to use every groove site either. If we use every other groove site in the y dimension, our grid will be much more

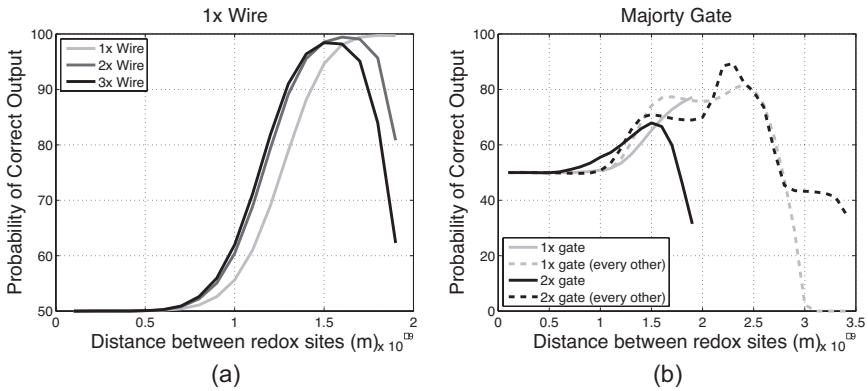

Fig. 9. Probability of a correct output as a function of the distance between redox sites with a DNA scaffolding. (a) considers wires and 0.9 nm between redox sites, (b) considers majority gates using every DNA grid spacing, and every other grid spacing in the y-dimension.

square—3.6 nm in the x, and 4.0 nm in the y dimension. Note that the variance between the x and y grid spacings is just 0.4 nm—results from the last section showed that circuits could be tolerant to this variation. The probability of a correct majority gate output, as a function of redox spacing, assuming a DNA scaffolding where every other grid spacing is used is also shown in Figure 9b. As one can see, for a device with approximately 2 nm between redox sites, the probability of a correct output is high.

Future work will also consider the following two threads. First, although the DNA double helix is 2.1 nm in diameter, electrostatic repulsion between adjacent DNA helices can lead to larger separations between adjacent helices. At high coverages, linear DNA could adopt a "fingerprint" pattern on surfaces, with DNA-DNA separations of 4 nm (i.e., a grid that is more naturally square). Second, when considering excess charge, the charge associated with a DNA scaffolding may be greater than the charge of one electron-making the probability of a correct output decrease. Alternatively, charge screening may reduce the impact of background charge, or cause charged DNA to been seen by the QCA molecules as a more diffuse charge with a weaker magnitude. This might increase the probability of a correct output. We are currently working with chemists to refine our charge models, and get more insight into how this substrate might affect logic.

8. CONCLUSIONS

This work not only provides a foundation for other systems-level study of molecular QCA devices, but it also offers insights that are useful for physical scientists attempting to develop molecular QCA systems. It leverages a still evolving simulation suite to better account for mistake states in a molecular implementation of QCA. Results illustrate that we need to consider devices, scaffoldings, and circuits simultaneously—or we may run the risk of creating devices that work only in isolation. Experimentally, fabricating and placing just one device is a significant challenge. It makes sense

to try to fabricate and place a device that will actually lead to circuits and systems.

The foundation created by this work will also inform computer scientists as to which implementation issues also require insight at the systems-level. For example, how will expected defects affect logic? Must architectures compensate? Will added device-level redundancy to combat defects add more switching events and degrade performance wins? Many of these questions only have answers at the systems-level. Answering them will help determine the viability of an emerging technology. By utilizing simulation tools with practical simulation parameters, we can begin to answers these questions.

Our results suggest the following: (1) future work should carefully consider the distribution of stray charge that might be associated with potential patterning mechanisms. (Specific grid spacings should be studied too.) This work should impact the design of molecules as well as the design of circuits and architectures. For example, it can help determine the desired height of a molecule's "feet" and will impact required circuit-level and architectural redundancy. Circuit layout may be affected too if the charge distribution is more predictable—as with DNA—we may be able to route logic around potential trouble spots. (2) An inverter is a good benchmark to consider among the constructs needed for a functionally complete logic set. If the inverter shows a high probability of producing a correct output, other logic elements should work too—allowing us to dedicate simulation cycles to more fine grained modeling. Tests performed on the logic elements should be simulated within the context of realistic grid spacings. (3) Manufacturing tolerances should be established by computer scientists looking at basic logic design and a functionally complete logic set. Insight from such studies could shape experimental work by allowing physical scientists to sacrifice determinism in one dimension (i.e., rotation) for determinism in another (i.e., a molecule's height).

By considering how devices and scaffoldings will join to form logic, the design community has the opportunity to push back on physical science—quite possibly having a direct effect on actual experiments. CAD can guide experimentalists with regard to how devices should be made, what their dimensions ideally should be to facilitate logic, circuits, and functional units, what scaffolding capabilities should be targeted, and what device-level redundancy is required. Additionally, design is an excellent vehicle to determine the eventually viability of QCA—not from a manufacturing perspective, but from a performance perspective. Understanding how manufacturing defects affect logic will ultimately allow for system architectures to evolve which will in turn allow us to generate realistic performance estimates for area, latency, and power. We can use these results to determine whether or not QCA can really provide the performance that some applications may need [DeBenedictis 2005]. (For example, determining required device-level redundancy will impact the number of switching events which will impact power dissipation.)

Ongoing work includes (1) modifying our simulation engine to consider tilts, shifts, and rotations in all three dimensions, (2) working with collaborators to create a clock driven 6-state simulator, (3) considering charge mappings of

candidate substrates, and (4) leveraging experimental results for more accurate defect rates.

ACKNOWLEDGMENTS

We thank Dan Gezelter for helpful conversations.

REFERENCES

AMLANI, I., ORLOV, A., SNIDER, G., AND LENT, C. 1998. Demonstration of a functional. quantum-dot cellular automata cell. *J. Vac. Sci. Tech. B. 16*, 3795–99.

BLAIR, E. P. 2003. Tools for the design and simulation of clocked molecular quantum-dot cellular automata circuit. M.S. thesis, University of Notre Dame.

CHAUDHARY, A., CHEN, D., HU, X., NIEMIER, M., RAVICHANDRAN, R., AND WHITTON, K. 2005. Eliminating wire crossings for molecular quantum-dot cellular automata implementation. In *Proceedings of the International Conference on Computer-Aided Design*, 565–571.

CREUTZ, C. AND TAUBE, H. 1973. Binuclear complexes of ruthenium ammines. *J. Amer. Chem. Soc. 95,* 4, 1086–1094.

DEBENEDICTIS, E. 2005. Reversible logic for supercomputing. In *Proceedings of 2nd Conference of Computer Frontiers*, 391–402.

HENNESSY, K. AND LENT, C. 2001. Clocking of molecular quantum-dot cellular automata. *J. Vac. Sci. Tech. B 19*, 5, 1752–1755.

HU, W., SARVESWARAN, K., LIEBERMAN, M., AND BERNSTEIN, G. H. 2005. High resolution electron beam lithography and DNA nano-patterning for molecular QCA. *IEEE Trans. Nanotech. 4*, 312–316.

HURLEY, D. AND TOR, Y. 2002. Ru(II) and Os(II) nucleosides and oligonucleotides: Synthesis and properties. *J. Amer. Chem. Soc. 124*, 3749–3762.

IMRE, A., CSABA, G., JI, L., ORLOV, A., BERNSTEIN, G., AND POROD, W. 2006. Majority logic gate for magnetic quantum-dot cellular automata. *Science 311*, 5758, 205–208.

JIAO, J., LONG, G., GRANDJEAN, F., BEATTY, A., AND FEHLNER, T. 2003. Building blocks for the molecular expression of quantum cellular automata. isolation and characterization of a covalently bonded square array of two ferrocenium and two ferrocene complexes. *J. Amer. Chem. Soc. 125*, 1522–1523.

LABEAN, T., PARK, S., AHN, S., AND REIF, J. 2005. Stepwise dna self-assembly of fixed-size nanostructures. In *Foundations of Nanoscience, Self-Assembled Architectures, and Devices*, 179–181.

LE, J. D., PINTO, Y., SEEMAN, N., MUSIER-FORSYTH, K., TATON, T., AND KIEHL, R. 2004. DNA-templated self-assembly of metallic nanocomponent arrays on a surface. *Nanotech. Lett. 4*, 12, 2343–2347.

LENT, C. AND TOUGAW, P. 1997. A device architecture for computing with quantum dots. In *Proceedings of the IEEE 85*, 541.

NIEMIER, M., CROCKER, M., HU, X. S., AND LIEBERMAN, M. November 8, 2006. Using CAD to shape experiments in molecular QCA. In *Proceedings of the International Conference on Computer-Aided Design*, 907–914.

NIEMIER, M. AND KOGGE, P. 2001. Exploring & exploiting wire-level pipelining in emerging technologies. In *Proceedings of International Symposium on Computer Architecture*, 166–177.

QI, H., SHARMA, S., LI, Z., SNIDER, G., ORLOV, A., LENT, C., AND FEHLNER, T. 2003. Molecular quantum cellular automata cells. electric field driven switching of a silicon surface bound array of vertically oriented two-dot molecular quantum cellular automata. *J. Amer. Chem. Soc. 125*, 15250–15259.

ROTHEMUND, P. 2005. Design of DNA origami. In *Proceedings of the International Conference on Computer-Aided Design*. 471–478.

ROTHEMUND, P. W. K., PAPADAKIS, N., AND WINFREE, E. 2004. Algorithmic self-assembly of DNA sierpinski triangles. *PLOS Biology 2*, 2041–2053.

SNIDER, G., ORLOV, A., AMLANI, I., BERNSTEIN, G., LENT, C., MERZ, J., AND POROD, W. 1999. Quantum-dot cellular automata: Line and majority gate logic. *Japanese J. Appl. Phys. 38*, 7227–7229.

TIMLER, J. AND LENT, C. 2002. Power gain and dissipation in quantum-dot cellular automata. *J. Appl. Phys. 91*, 823–831.

TOUGAW, P. AND LENT, C. 1994. Logical devices implemented using quantum cellular automata. *J. Appl. Phys. 75*, 1818.

UNGARELLI, C., FRANCAVIGLIA, S., MACUCCI, M., AND IANNACCONE, G. 2000. Thermal behavior of quantum cellular automaton wires. *J. Appl. Phys. 87*, 10, 7320–7325.

WALUS, K., DIMITROV, V., JULLIEN, G., AND MILLER, W. Oct. 2003. QCADesigner: A cad tool for an emerging nano-technology. *Micronet An. Work. 2003*.

WANG, Y. AND LIEBERMAN, M. Sept. 2004. Thermodynamic behavior of molecular-scale quantum-dot automata (QCA) wires and logic devices. *IEEE Trans. Nanotech. 3*, 3, 368–376.

WINFREE, E., LIU, F., WENZLER, L., AND SEEMAN, N. 1998. Design and self-assembly of two-dimensional DNA crystals. *Nature 394*, 539–544.

Received July 2007; accepted September 2007